

See discussions, stats, and author profiles for this publication at: <https://www.researchgate.net/publication/41100984>

Facilitation of NADH Electro-oxidation at Treated Carbon Nanotubes

ARTICLE *in* ANALYTICAL CHEMISTRY · FEBRUARY 2010

Impact Factor: 5.64 · DOI: 10.1021/ac902301b · Source: PubMed

CITATIONS

73

READS

27

2 AUTHORS:



Marilyn Wooten

Trinity University

7 PUBLICATIONS 211 CITATIONS

SEE PROFILE



Waldemar Gorski

University of Texas at San Antonio

55 PUBLICATIONS 2,136 CITATIONS

SEE PROFILE

Published in final edited form as:

Anal Chem. 2010 February 15; 82(4): 1299. doi:10.1021/ac902301b.

Facilitation of NADH Electrooxidation at Treated Carbon Nanotubes

Marilyn Wooten and Waldemar Gorski*

Department of Chemistry, University of Texas at San Antonio, San Antonio, Texas 78249-0698

Abstract

The relationship between the state of the surface of carbon nanotubes (CNT) and their electrochemical activity was investigated using the enzyme cofactor dihydronicotinamide adenine dinucleotide (NADH) as a redox probe. The boiling of CNT in water, while nondestructive, activated them toward the oxidation of NADH as indicated by a shift in the anodic peak potential of NADH (E_{NADH}) from 0.4 to 0.0 V. The shift in E_{NADH} was due to the redox mediation of NADH oxidation by traces of quinone species that were formed on the surface of treated CNT. The harsher treatment that comprised of microwaving of CNT in concentrated nitric acid had a similar effect on the E_{NADH} and, additionally, it increased the anodic peak current of NADH. The latter correlated with the formation of defects on the surface of acid-microwaved CNT as indicated by their Raman spectra. The increase in current was discussed considering a role of surface mediators on the buckled graphene sheets of acid-microwaved CNT. The other carbon allotropes including the edge plane pyrolytic graphite, graphite powder, and glassy carbon did not display a comparable activation toward the oxidation of NADH.

Introduction

The electrooxidation of dihydronicotinamide adenine dinucleotide (NADH) is of great interest because hundreds of dehydrogenase enzymes rely on the NAD^+/NADH coenzyme couple. The efficient recycling of the NAD^+/NADH system is essential, for example, in the operation of a variety of electrochemical biosensors that are based on the NAD^+ -dependent dehydrogenase enzymes. However, the oxidation of NADH is slow at conventional electrodes and takes place only at high overpotentials. For example, although the formal potential of the NAD^+/NADH couple is low -0.56 V vs. SCE at pH 7.0, 25 °C)¹ the electrooxidation of NADH at carbon electrodes requires typically more than 1.0 V of overpotential. Furthermore, the oxidation of NADH at high potentials usually leads to fouling of the electrode surface, which diminishes the stability of the NADH current.

The initial attempts to overcome these limitations have concentrated on the use of redox mediators such as quinones,^{2–5} diamines,^{6,7} and phenazine and phenoxazine dyes^{8–14} to recycle the NADH back to the enzymatically active NAD^+ . The activity of these mediators toward the NADH oxidation has been explained in terms of a hydride transfer mechanism in which the mediator accepts the hydride and has the ability to delocalize the electrons.⁷ The oxidation of NADH has also been investigated using ferrocenes,^{4,15} transition metal complexes,^{16,17} conductive polymers,^{18–21} nitrofluorenone derivatives,^{22,23} dichloroindophenol,^{24–26} and tetracyanoquinodimethane-tetrathiafulvalene.²⁷ However, such

Corresponding author: (fax) 210-458-7428; waldemar.gorski@utsa.edu.

SUPPORTING INFORMATION AVAILABLE

Additional information as noted in the text. This material is available free of charge via the Internet at <http://pubs.acs.org>.

mediator-based electrodes have displayed intrinsic difficulties, which were related to the limited stability of mediators and their leaching from the electrodes.

The recent approaches to the facilitated oxidation of NADH included the use of electrodes based on different forms of carbon e.g. carbon nanotubes (CNT)^{11, 28–41} and pyrolytic graphite.⁴² Such materials significantly decreased the NADH overpotential, which was ascribed to the edge plane sites/defects present in the pyrolytic graphite and suspected in CNT.⁴³

The present paper demonstrates that further decrease in the NADH overpotential can be achieved at CNT that were activated by heating in deionized water under normal pressure. The electrochemical, spectroscopic, and microscopic analyses are used in order to explain the reasons for such activation. In addition, the oxidation of NADH at CNT is contrasted with that at other carbon allotropes including the edge plane pyrolytic graphite (EPPG), graphite powder (GP), and glassy carbon (GC).

EXPERIMENTAL SECTION

Reagents

Multiwalled carbon nanotubes (CNT, synthesized by the chemical vapor deposition, ~95 % nominal purity) were purchased from Nanolab (Brighton, MA). The CNT had a diameter of 15 ± 5 nm and length of 1–5 μm . Three batches of CNT purchased between 2004 and 2008 were used in the present studies. The edge plane pyrolytic graphite (EPPG, 1.0-mm-diameter rod), graphite powder (GP, 2–15 μm diameter), glassy carbon (GC, 3.0-mm-diameter rod), and 0.50-mm-diameter platinum wire were purchased from Alfa Aesar. Chitosan (CHIT, MW $\sim 1 \times 10^6$ Da; ~80 % deacetylation), dihydronicotinamide adenine dinucleotide (NADH), methanol, and ethanol were purchased from Sigma-Aldrich. The $\text{NaH}_2\text{PO}_4 \cdot \text{H}_2\text{O}$, Na_2HPO_4 , HCl, HNO_3 , and NaOH were from Fisher. The chitosan solutions were prepared by dissolving chitosan flakes in hot (90 °C) aqueous solutions of 0.05 M HCl and filtering with a syringe filter.⁴⁴ All solutions were prepared using 18-M Ω -cm deionized water that was purified with a Barnstead NANOpure cartridge system.

Treatment of CNT and Other Carbon Allotropes

The CNT were either boiled in deionized water at normal pressure for 10–30 min or microwaved in a concentrated nitric acid (70%) for 10–20 min. The microwaving was performed at 50 °C, 20 psi, and 100% power using the Discover Labmate® single mode microwave oven (CEM, 300 W). After the boiling or microwaving, the CNT were subjected to at least three centrifugation/decanting cycles in fresh aliquots of deionized water in order to remove any remaining impurities. In addition, the acid-treated CNT suspensions were neutralized with a sodium hydroxide solution and washed extensively with water to a neutral pH. The final rinsing was performed with ethanol. The CNT were dried in an oven at 85 °C overnight and stored in closed vials at room temperature.

The EPPG, EG, and GC were microwaved in the concentrated nitric acid (70%), rinsed with water, and dried at 85 °C overnight. The EPPG and GC rods were wrapped with a Teflon tape to expose only the disc area to a solution during the electrochemical measurements.

Preparation of Film Electrodes

The film electrodes were prepared by casting 10 μL of suspension of 1.0 mg CNT (or GP) in 1.0 mL of 0.010 wt. % chitosan solution on the surface of a 3.0-mm-diameter GC disk electrode (Bioanalytical Systems, Inc.; BAS) and dried for 2 h at room temperature. The film electrodes were rinsed repeatedly with water and soaked in a pH 7.40 phosphate buffer solution while

stirring in order to remove any loose materials. The electrodes were stored covered at room temperature when not in use.

Electrochemical Measurements

A CHI 832B workstation (CH Instruments, Inc.) was used to collect electrochemical data. The measurements were performed in the three-electrode system using a Faraday cage (Bioanalytical Systems, Inc.; BAS). The carbon electrodes served as a working electrode, a platinum wire was used as the auxiliary electrode, and the reference electrode was the Ag/AgCl/3MNaCl (BAS). The GC and EPPG electrodes were wet polished on an Alpha A polishing cloth (Mark V Lab) with successively smaller particles (0.3 and 0.05 μm diameter) of alumina. The alumina slurry was removed from the electrode surface by the ultrasonication in deionized water and methanol.

All experiments were performed at room temperature (20 ± 1 °C) using deoxygenated pH 7.40 phosphate buffer solution (0.10 M) as a background electrolyte. The experiments were repeated minimum three times and the means of measurements are presented with the relative standard deviation.

Spectroscopic, Microscopic, and Thermogravimetric Measurements

The Raman spectra of CNT were collected using a Jovin-Yblon Horiba Labram 800 with the 632.8 nm emission line from a He-Ne laser (2.5 mW) with the path length of 0.80 m and the laser spot size of 2 μm diameter. The infrared (FTIR) spectra were collected with a Bruker Equinox 55 spectrometer. The thermogravimetric analysis (TGA) was performed with a TGA-50 thermogravimetric analyzer (Shimadzu). The experiments were carried out in an atmosphere of flowing air (10 mL min^{-1}) at a heating rate of 20 °C min^{-1} . Energy dispersive X-Ray (EDX) analysis was performed with a High-Angle Annular Dark-Field (HAADF)-Scanning Electron Microscope (SS-Hitachi 5500 STEM). The morphology and composition of treated carbon nanotubes were investigated by using the high resolution transmission electron microscopy (HRTEM) and scanning transmission electron microscopy (STEM) in conjunction with the electron energy loss spectroscopy (EELS). An aliquot of ethanol-suspended carbon nanotubes was placed onto a carbon-coated TEM grid and dried at room temperature. The analysis was performed with a Schottky field-emitter-based FEI Tecnai TF20 (200kV) outfitted with a STEM unit, HAADF detector, and X-Twin lenses (Supplemental Information).

RESULTS AND DISCUSSION

Electrooxidation of NADH at Original and Treated CNT

Figure 1 shows the cyclic voltammograms recorded at the glassy carbon electrodes that were modified with the original CNT (A), water-boiled CNT (B), and acid-microwaved CNT (C). The voltammograms were recorded in the presence and absence of NADH in a solution as illustrated by traces 1 and 2, respectively. The boiling of CNT in water for 30 min resulted in a dramatic shift of the oxidative peak potential of NADH (E_{NADH}) to a lower value, from approx. 0.38 V (trace A1) to 0.0 V (trace B1). Similar effect was also observed with the CNT that were microwaved in a concentrated nitric acid (70%) solution for 20 min (trace C1). The peak C1 displayed features of the electrode process from the adsorbed state. All three batches of CNT purchased from Nanolab between 2004 and 2008 yielded similar voltammetric results with a standard deviation for E_{NADH} not larger than ± 0.03 V. Table 1 summarizes the effects of different treatment of CNT on E_{NADH} . In the case of water-boiled CNT, the E_{NADH} correlated directly with the pretreatment time and its value stabilized at 0.0 V after 30 min of boiling. Only 10–20 min of CNT microwaving in acidic solution was required to shift the E_{NADH} to -0.04 V, while the sonication of CNT in acidic solution shifted the E_{NADH} to -0.01

V. In contrast to boiling in water, the microwaving of CNT in nitric acid removed the Fe catalyst that was used in their synthesis.^{36,37} Thus, the metal catalyst seems to be not responsible for the shift in E_{NADH} considering that the shift was approximately to the same value (0.0 V) at both the water-boiled and acid-microwaved CNT.

The shift in E_{NADH} correlated with the appearance of a distinct pair of current peaks in the background voltammograms B2 and C2 at approx. -0.07 V (Figure 1). The analogous pair of current peaks has been observed before at the CNT that were sonicated in 3 M nitric acid for 7 h at room temperature.³⁵ These current peaks have been ascribed to the redox active quinones that were formed on the surface of acid-sonicated CNT. Apparently, our much shorter treatments of CNT generated similar carbon-oxygen functionalities on the surface of CNT. Thus, the shift in E_{NADH} illustrated in Figure 1 and Table 1 can be attributed to the redox mediation of NADH oxidation by surface quinones^{2,3}



which is followed by the recycling of quinone species on the surface of treated CNT



Since the reactions 1 and 2 are faster than the direct electrooxidation of NADH to NAD^+ , the mediated process (1)-(2) allows converting the NADH to NAD^+ at less positive potentials close to the formal potential of the Q/QH_2 redox couple (-0.07 V). One can hypothesize that the surface species facilitate the transfer of hydride and delocalization of electrons from the NADH to the treated CNT. The mediation hypothesis is supported by the fact that the anodic surface peak is enhanced while the cathodic surface peak is diminished in the presence of NADH in a solution (Figures 1B and 1C).

The integration of the background peaks at -0.07 V (Figure 1) yielded a concentration of the redox active species equal to $2.0 \times 10^{-10} \text{ mol cm}^{-2}$ ($\pm 10\%$, $N=4$) and $2.7 \times 10^{-10} \text{ mol cm}^{-2}$ ($\pm 25\%$, $N=3$) on the surface of water-boiled (trace B2) and acid-microwaved (trace C2) CNT, respectively. These calculations were done assuming a 2e^- surface reaction 2 and using a surface area of a glassy carbon disk. It should be pointed out, however, that the surface concentrations obtained in this way were very sensitive to the amount of CNT placed on the surface of glassy carbon electrodes.

A rather peculiar behavior was observed in the case of the direct oxidation of NADH at the electrodes modified with the original CNT (Figure 1A). The voltammogram in this case changed from a typical peak-shaped plot in the presence of oxygen in a solution⁴⁵ to a sigmoidal voltammogram in the absence of oxygen (trace A1). The origin of this change is not clear at present but it can reflect, in the absence of oxygen, the lack of a peak-causing depletion of NADH at CNT on the time scale of the experiment.

The literature survey of the effects of CNT treatment on E_{NADH} revealed a degree of inconsistency. The following are the recent examples of such effects in the case of CNT that were all synthesized by the chemical vapor deposition. In one case, the low-potential oxidation of NADH has been achieved at the CNT that were sonicated in 3 M nitric acid for 7 h ($E_{\text{NADH}} = 0.01$ V, pH 7.2, 5.0 mV s^{-1}).³⁵ The other case involved the ordered CNT that were synthesized within the pores of alumina membrane, annealed at 720°C , treated in 0.10 M HCl, and used as a free-standing membrane after dissolution of alumina in concentrated sodium hydroxide solution ($E_{\text{NADH}} = 0.04$ V, pH 6.80, 50 mV s^{-1}).³⁹ Both groups ascribed the shift in E_{NADH} to the presence of carbon-oxygen species on the surface of their CNT. A different

study reported that the electrooxidation of super-long vertically aligned CNT at 1.8 V for 3 min in pH 6.5 phosphate buffer solution shifted the E_{NADH} from 0.60 to 0.15 V (pH 6.5, 100 mV s^{-1}).³⁰ Yet another study concluded that the electrooxidation of CNT at 1.75 V for 3 min in pH 7.4 phosphate buffer solution had no effect on E_{NADH} ($E_{\text{NADH}} = 0.19$ V before and after the treatment, pH 7.40, 100 mV s^{-1}).³⁸

Electrooxidation of NADH at Other Carbon Allotropes

The values of E_{NADH} were determined using the cyclic voltammograms, which were recorded at 5 mV s^{-1} at the electrodes made of different carbon allotropes (not treated). The E_{NADH} was slightly higher at the electrodes made of the original EPPG (0.40 V) than at the original CNT (0.38 V), which was consistent with the recent literature reports.⁴³ The value of E_{NADH} increased further at the electrodes made of GP (0.54 V) and GC (0.70 V), which suggested a more difficult electrode process at these surfaces. These differences in E_{NADH} can be ascribed, at least partially, to the differences in the density of electronic states and carrier density in the carbon allotropes.^{46,47} In particular, following the existing literature,^{47,48} this trend can be tentatively attributed to a decreasing density of active edge plane sites in the order $\text{CNT} \geq \text{EPPG} > \text{GP} > \text{GC}$.

In contrast to CNT, the microwaving of EPPG in nitric acid resulted only in a minor shift in the E_{NADH} from 0.40 to 0.38 V. The acid-microwaved EPPG displayed very small surface peaks in the background cyclic voltammograms at 0.0 V (not shown). The integration of these current peaks yielded a concentration of the redox active species equal to $4 \times 10^{-11} \text{ mol cm}^2$ ($\pm 25\%$, $N=3$) on the surface of acid-microwaved EPPG. Apparently, these surface species were not mediating the oxidation of NADH efficiently enough to cause a larger shift in the E_{NADH} . One can hypothesize that the lower concentration of redox active species on EPPG resulted from a smaller density of reactive edge plane sites on the surface of EPPG than in the three-dimensional films of CNT.

There was also practically no shift in the E_{NADH} at the electrodes made of acid-microwaved GP. This correlated with the absence of any measurable current peaks at 0.0 V in the background voltammograms of such electrodes.

The electrodes made of GC were an exception because they displayed a substantial shift in E_{NADH} from 0.70 to 0.50 V after microwaving in nitric acid although no detectable current peaks at 0.0 V were observed in the background voltammograms of acid-microwaved GC electrodes. The shift 0.70 V \rightarrow 0.50 V can be ascribed to the desorption of impurities from the surface of the treated GC electrodes.⁴⁷ The microwaving of EPPG, GP, and GC had a minimal effect on the NADH peak currents.

The foregoing discussion shows that the selection of a carbon allotrope greatly affects the value of E_{NADH} (GC, 0.70 V; GP, 0.54 V; EPPG, 0.40 V; CNT, 0.38 V). In contrast to the GC, GP, and EPPG, the treatment of CNT further lowers the E_{NADH} to 0.0 V. However, even this potential (0.0 V, pH 7.40) is still far from the thermodynamic potential of the NAD^+/NADH system (-0.52 V vs. $\text{Ag}/\text{AgCl}/3\text{MNaCl}$, pH 7.0).

Amperometric Determination of NADH at CNT

Figure 2 presents the amperometric traces recorded at -0.050 V at the CNT-modified electrodes during the spiking of NADH aliquots into a stirred buffer solution. At such a low potential, the electrodes based on the original CNT displayed no detectable current due to the oxidation of NADH (trace a). The electrodes modified with water-boiled CNT displayed a distinct NADH signal in the form of current steps after each addition of NADH to the solution (trace b). The analysis of these steps yielded the detection limit of $4.0 \mu\text{M}$ NADH, sensitivity of 3.2 mA

$\text{M}^{-1} \text{cm}^{-2}$ (disk area), response time of ~ 10 s, dynamic range from $10 \mu\text{M}$ to 10mM , and the linear range from 10 to $100 \mu\text{M}$ ($R^2 = 0.995$).

Consistent with the higher NADH peak currents at electrodes based on the acid-treated CNT (Figure 1, trace C1), such electrodes showed higher amperometric response to NADH (Figure 2, trace c). The acid-treated CNT yielded the detection limit of $2.0 \mu\text{M}$ NADH, sensitivity of $12 \text{mA M}^{-1} \text{cm}^{-2}$ (disk area), response time of ~ 50 s, dynamic range from $10 \mu\text{M}$ to 10mM , and the linear range from 10 to $100 \mu\text{M}$ ($R^2 = 0.993$).

The operational stability studies indicated that the electrodes based on the treated CNT were the most stable and retained approx. 70 % of the initial current after 1.5 h of continuous operation at -0.05V in a stirred solution (800 rpm) of 0.10mM NADH. The interferences studies showed that the ascorbic acid (0.10mM) interfered with the determination of 1.0mM NADH at -0.05V . The determination of NADH was not affected by the 0.10mM concentrations of other potentially interfering species such as the acetaminophen and uric acid.

Non-Electrochemical Studies of Original and Treated CNT

The relationship between the state of CNT surface and its electrochemical activity was further studied by using a set of non-electrochemical techniques. The initial observations showed that both the water-boiled and acid-microwaved CNT could be dispersed in water much easier than the original CNT. While the latter precipitated quickly, the treated CNT formed dark stable suspensions in water (Figure 1S). This suggested that the surface of treated CNT became more hydrophilic than that of the original CNT.

The hydrophilicity of the treated CNT has been ascribed before to the formation of carboxylic groups on the surface of CNT.⁴⁹ However, the acid-base back titrations of the CNT suspensions could not detect the acidic groups on the surface of the treated CNT. This was consistent with a recent report, which indicated that the acid-base titration could detect the carboxylic groups as dominant surface species only after long (6 h) oxidation of CNT in the concentrated nitric acid.⁴⁹ Apparently, the carboxylic groups were not the dominant species among the carbon-oxygen groups on the surface of CNT that were subjected to our relatively short (30 min) treatments.

The EDX and FTIR analyses of the treated CNT showed that the oxygen signals were below the detection limit of these techniques (not shown). The EELS analysis also displayed no oxygen signal at the expected 540eV position in the spectra of treated CNT. These results are compatible with the recent reports, which argue that the mild treatments of CNT (e.g. sonication of CNT in water at room temperature)⁵⁰ result in the formation of just traces of carbon-oxygen functionalities such as $-\text{OH}$, $-\text{C}=\text{O}$, and $-\text{COOH}$ on the surface of CNT. At present, only the electrochemistry (Figures 1B and 1C, lines 2) and the formation of aqueous suspensions (Figure 1S) provide the supportive arguments for the presence of carbon-oxygen species on the surface of our treated CNT.

The HRTEM images (Figures 2SA and 2SB) showed that there were no drastic differences in the surface morphology of the original and water-boiled CNT. However, the surface of the acid-microwaved CNT displayed a degree of surface disruption in the form of buckled graphene walls (Figure 3).

The Raman analysis of CNT supported the HRTEM observations. Figure 4 shows the Raman spectra of the original (a), water-boiled (b), and acid-microwaved CNT (c). The spectra are composed of two characteristic bands at 1328cm^{-1} (D band) and 1578cm^{-1} (G band), and a shoulder at 1601cm^{-1} (D' band). The D band is a measure of structural disorder^{47,51–53} coming from any surface defects such as the edges, finite size effects, and impurities that break

the translational symmetry (no detectable amorphous carbon impurities were indicated by the HRTEM and thermogravimetric analyses of our samples). The G band is a measure of the stretching vibrations of the carbon-carbon bonds within the graphene sheets.^{47,51–53} Similar to the D band, the D' band is a double-resonance Raman feature that originates from the disorder due to the defects or ion intercalation. The D' band is absent in the Raman spectra of pure graphite but it is highly intense in the spectra of intercalated graphite.⁵⁴ Figure 4 shows that a distinct D' band is present only in the spectrum of the acid-sonicated CNT suggesting that the sonication in the nitric acid solution promoted the intercalation of ions into CNT.

The integrated intensity ratio of the D and G bands, $R = I_D/I_G$, of many crystalline graphitic materials has been shown to be inversely proportional to the in-plane crystallite sizes L_a obtained from the analysis of X-ray diffraction peaks of such materials ($L_a \approx R^{-1}$).⁵⁵ Based on the data in Figure 4, the ratio R for the original, water-boiled, and acid-microwaved CNT was equal to 0.68, 0.76, and 1.5, respectively. The conversion of the R values into the L_a sizes was done by using the equation⁵⁶

$$L_a \text{ (nm)} = (2.4 \times 10^{-10}) \lambda_1^4 R^{-1} \quad (3)$$

(λ_1 is the laser line wavelength in nm) and yielded the values of 57, 50, and 26 nm for the original, water-boiled, and acid-microwaved CNT, respectively. This implied that the density of defects in the films of water-boiled CNT was only 1.1 times larger than that in the original CNT. Apparently, the boiling of CNT in water was only minimally destructive. On the other hand, the density of defects was almost 2 times larger in acid-microwaved CNT than in the water-boiled CNT.

The foregoing analysis allows for the following observations. First, the surface defects played a rather negligible role in the large shift of E_{NADH} from 0.40 V (at the original CNT) to 0.0 V (at the water-boiled CNT). The primary cause of this shift was the mediation of the NADH oxidation by the redox-active groups on the surface of the water-boiled CNT. Second, the increase in surface defects in the acid-microwaved CNT did not cause any further significant shift in E_{NADH} , which stayed close to 0.0 V at both the water-boiled and acid-microwaved CNT. Third, the increase in the density of surface defects in the acid-microwaved CNT correlated with the increase in the NADH peak current (Figure 1, curve C1). One can hypothesize that this correlation reflected a combination of effects including the enhanced adsorption of NADH at defect sites and faster mediation kinetics due to a better access of NADH molecules to the mediator species on a corrugated surface of acid-microwaved CNT (Figure 3).

CONCLUSIONS

In contrast to other carbon allotropes such as the glassy carbon, graphite powder, and edge plane pyrolytic graphite, the multiwalled CNT with a nominal purity of 95% (Nanolab) required only a relatively short and mild treatment in order to introduce the surface redox mediators, which drastically reduced (by 0.4 V) the overpotential for the electrooxidation of NADH. This underscored the advantage of CNT as an electrode material for the facilitated oxidation of NADH at low potentials. The variation in the values of the anodic peak potential for the NADH at the original (not treated) carbon allotropes could be tentatively attributed to a decreasing density of active edge plane sites on their surface ($\text{CNT}(0.38\text{V}) \geq \text{EPPG}(0.40\text{V}) > \text{GP}(0.54\text{V}) > \text{GC}(0.70\text{V})$).

Supplementary Material

Refer to Web version on PubMed Central for supplementary material.

Acknowledgments

This work was supported by the NIH/MBRS/SCORE Grant GM 08194 and The Welch Foundation Departmental Research Grant AX-0026. The authors gratefully acknowledge Dr. Domingo Ferrer (UT Austin) for collecting the EELS spectra and HRTEM images.

Bibliography

1. Gorton L. J. Chem. Soc., Faraday Trans. 1 1986;82:1245–1248.
2. Tse DC-S, Kuwana T. Anal. Chem 1978;50:1315–1318.
3. Carlson BW, Miller LL. J. Am. Chem. Soc 1985;107:479–485.
4. Antiochia R, Gallina A, Lavagnini I, Magno F. Electroanalysis 2002;14:1256–1261.
5. Ge B, Tan Y, Xie Q, Ma M, Yao S. Sens. Actuators, B 2009;B137:547–554.
6. Kitani A, So YH, Miller LL. J. Am. Chem. Soc 1981;103:7636–7641.
7. Kitani A, Miller LL. J. Am. Chem. Soc 1981;103:3595–3597.
8. Wang JW, Xia ZH, Chu JH, Tan RX. Enzyme Microb. Technol 2004;34:651–656.
9. Wu S-W, Huang HY, Guo YC, Wang CM. J. Phys. Chem. C 2008;112:9370–9376.
10. Schuhmann W, Huber J, Wohlschlaeger H, Strehlitz B, Gruendig B. J. Biotechnol 1993;271:129–142.
11. Lawrence NS, Wang J. Electrochem. Commun 2006;8:71–76.
12. Ohtani M, Kuwabata S, Yoneyama H. J. Electroanal. Chem 1997;422:45–54.
13. Zhang M, Gorski W. Anal. Chem 2005;77:3960–3965. [PubMed: 15987097]
14. Zhang M, Gorski W. J. Am. Chem. Soc 2005;127:2058–2059. [PubMed: 15713079]
15. Ramirez-Molina C, Boujtita M, El Murr N. Electroanalysis 2003;15:1095–1100.
16. Storrier GD, Takada K, Abruna HD. Inorg. Chem 1999;38:559–565. [PubMed: 11673962]
17. Wu Q, Maskus M, Pariente F, Tobalina F, Fernandez VM, Lorenzo E, Abruna HD. Anal. Chem 1996;68:3688–3696.
18. Manesh KM, Santhosh P, Gopalan A, Lee KP. Talanta 2008;75:1307–1314. [PubMed: 18585217]
19. Valentini F, Salis A, Curulli A, Palleschi G. Anal. Chem 2004;76:3244–3248. [PubMed: 15167808]
20. Bartlett PN, Simon E, Toh CS. Bioelectrochemistry 2002;56:117–122. [PubMed: 12009456]
21. Bartlett PN, Wallace ENK. J. Electroanal. Chem 2000;486:23–31.
22. Munteanu FD, Mano N, Kuhn A, Gorton L. J. Electroanal. Chem 2004;564:167–178.
23. Mano N, Kuhn A. Biosens. Bioelectron 2001;16:653–660. [PubMed: 11679241]
24. Lin W-J, Chen MH. Carbohydr. Polym 2007;67:474–480.
25. Rakhi RB, Sethupathi K, Ramaprabhu S. Nanoscale Res 2007;2:331–336.
26. Forrow NJ, Sanghera GS, Walters SJ, Watkin JL. Biosens. Bioelectron 2005;20:1617–1625. [PubMed: 15626617]
27. Pandey PC, Upadhyay S, Upadhyay BC, Pathak HC. Anal. Biochem 1998;260:195–203. [PubMed: 9657878]
28. Sanchez S, Fabregas E, Pumera M. Phys. Chem. Chem. Phys 2009;11:182–186. [PubMed: 19081922]
29. Kachoosangi RT, Musameh MM, Abu-Yousef I, Yousef JM, Kanan SM, Xiao L, Davies SG, Russell A, Compton RG. Anal. Chem 2009;81:435–442. [PubMed: 19117466]
30. Gong K, Chakrabarti S, Dai L. Angew. Chem., Int. Ed 2008;47:5446–5450.
31. Zhou M, Shang L, Li B, Huang L, Dong S. Electrochem. Commun 2008;10:859–863.
32. Zhou M, Shang L, Li B, Huang L, Dong S. Biosens. Bioelectron 2008;24:442–447. [PubMed: 18541421]
33. Zhu L, Tian C, Yang D, Jiang X, Yang R. Electroanalysis 2008;20:2518–2525.

34. Tsai Y-C, Tsai M-C, Chiu C-C. *Electrochem. Commun* 2008;10:749–752.
35. Chakraborty S, Raj CR. *J. Electroanal. Chem* 2007;609:155–162.
36. Wang Y, Iqbal Z, Mitra S. *J. Am. Chem. Soc* 2006;128:95–99. [PubMed: 16390136]
37. Lawrence NS, Deo RP, Wang J. *Electroanalysis* 2005;17:65–72.
38. Musameh M, Lawrence NS, Wang J. *Electrochem Comm* 2005;7:14–18.
39. Chen J, Bao J, Cai C, Lu T. *Anal. Chim. Acta* 2004;516:29–34.
40. Musameh M, Wang J, Merkoci A, Lin Y. *Electrochem. Comm* 2002;4:743–746.
41. Zhang M, Gorski W. *Anal. Chem* 2007;79:2446–2450. [PubMed: 17298031]
42. Moore RR, Banks CE, Compton RG. *Anal. Chem* 2004;76:2677–2682. [PubMed: 15144174]
43. Banks CE, Compton RG. *Anal. Sci* 2005;21:1263–1268. [PubMed: 16317891]
44. Zhang M, Mullens C, Gorski W. *Anal. Chem* 2005;77:6396–6401. [PubMed: 16194105]
45. Zhang M, Smith A, Gorski W. *Anal. Chem* 2004;76:5045–5050. [PubMed: 15373440]
46. Cline KK, McDermott MT, McCreery RL. *J. Phys. Chem* 1994;98:5314–5319.
47. McCreery RL. *Chem. Rev* 2008;108:2646–2687. [PubMed: 18557655]
48. Banks CE, Compton RG. *Analyst* 2005;130:1232–1239. [PubMed: 16096667]
49. Wang Z, Shirley MD, Meikle ST, Whitby RLD, Mikhlovsky SV. *Carbon* 2009;47:73–79.
50. Yang D-Q, Rochette J-F, Sacher E. *J. Phys. Chem. B* 2005;109:7788–7794. [PubMed: 16851905]
51. Wang Y, Alsmeyer DC, McCreery RL. *Chem. Mater* 1990;2:557–563.
52. Ray K, McCreery RL. *Anal. Chem* 1997;69:4680–4687.
53. Osswald SHM, Gogotsi Y. *J. Raman Spectrosc* 2007;38:728–736.
54. Solin SA, C. N. J. *Raman Spectrosc* 1981;10:129–135.
55. Baldan MRA, EC, Azevedo AF, Gocalves ES, Rezende MC, Ferreira NG. *Appl. Surf. Sci* 2007;254:600–603.
56. Cançado LGT, K, Enoki T, Endo M, Kim YA, Mizusaki H, Jorio A, Coelho LN, Magalhães-Paniago R, Pimenta MA. *Appl. Phys. Lett* 2006;88:1631061–1631063.

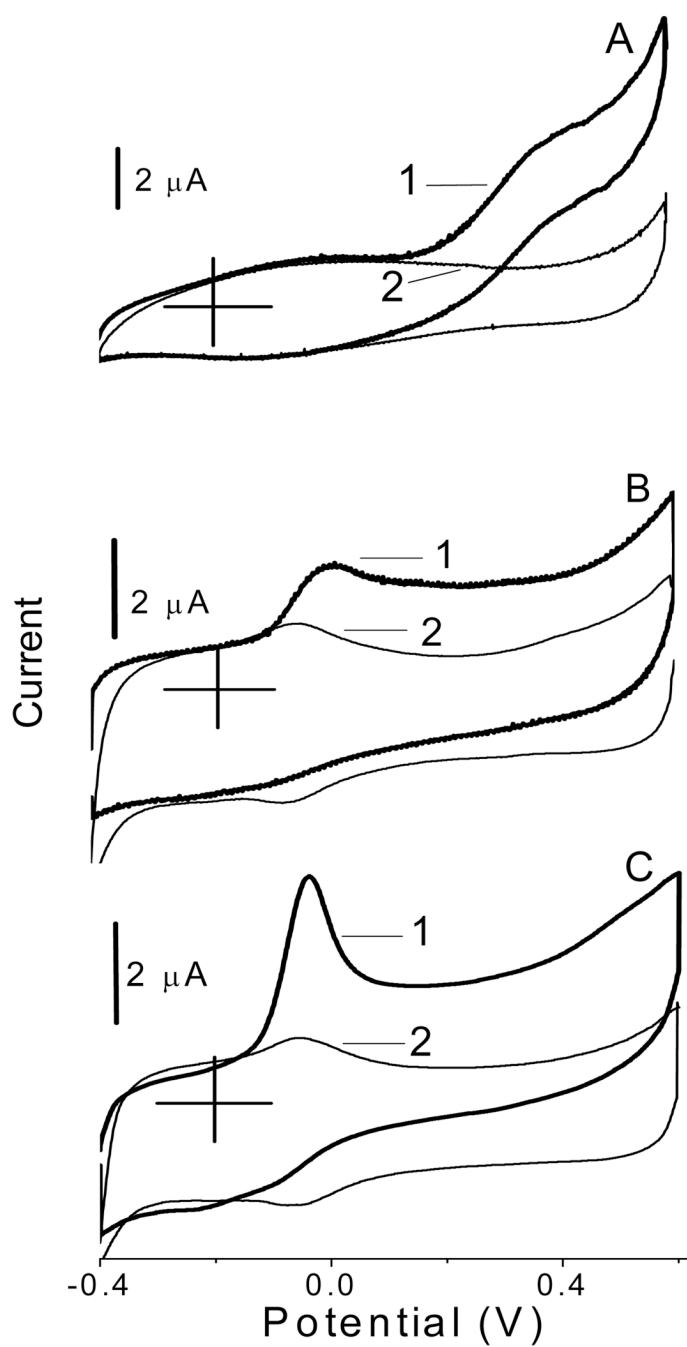


Figure 1.

Cyclic voltammograms recorded at the glassy carbon electrodes that were modified with the original (A), water-boiled (B), and acid-microwaved (C) CNT in deoxygenated solutions with (1) and without (2) 1.0 mM NADH. Background electrolyte, 0.05 M phosphate buffer solution at pH 7.40. Scan rate, 5.0 mV s^{-1} .

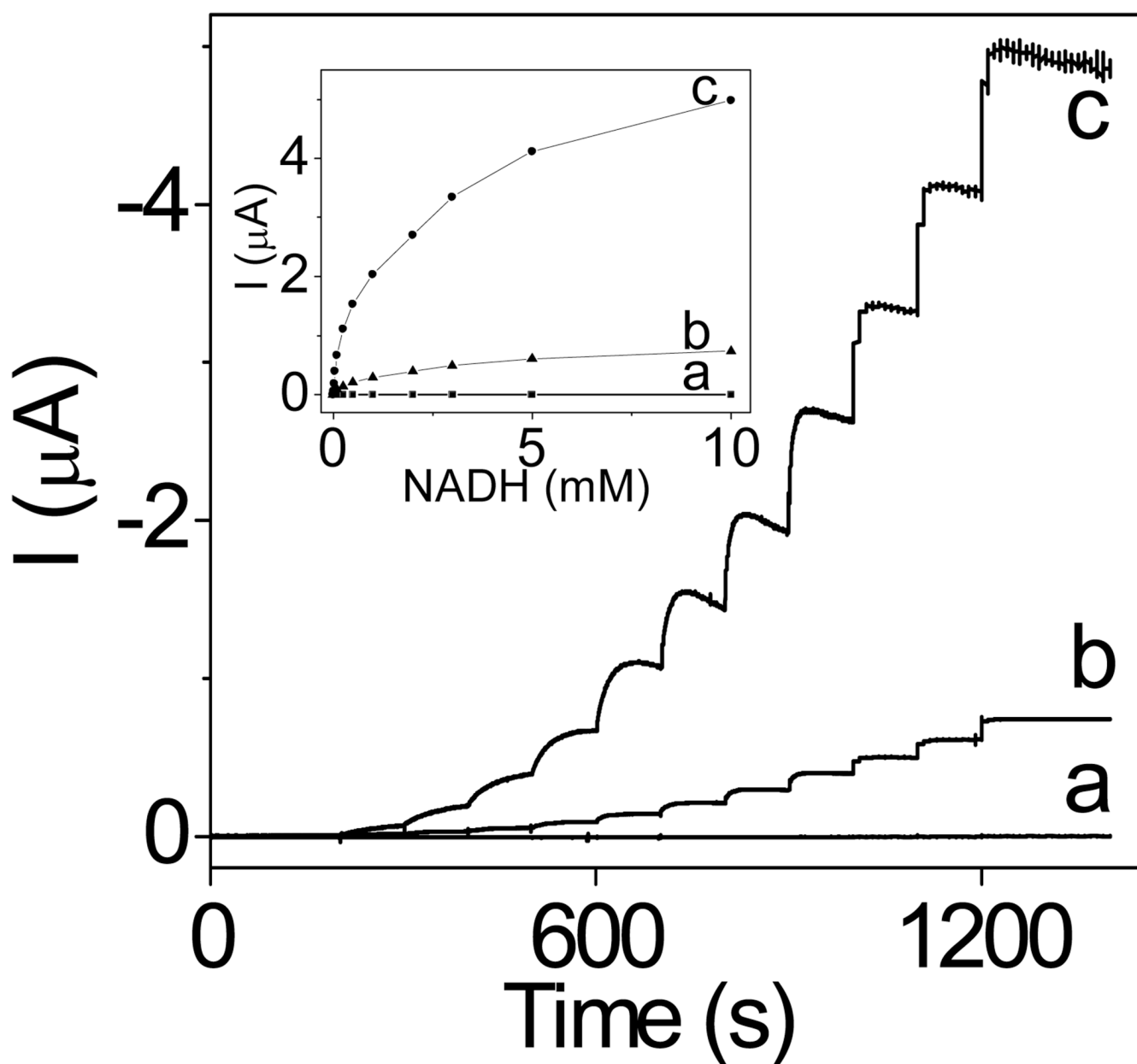


Figure 2. Amperometric responses ($E = -0.05\text{V}$) of the glassy carbon electrodes modified with the original (a), water-boiled (b), and acid-microwaved (c) CNT to additions of NADH aliquots. The current steps correspond to 0.010, 0.025, 0.050, 0.10, 0.25, 0.50, 1.0, 2.0, 3.0, 5.0, and 10.0 mM NADH. Inset: The related calibration curves.

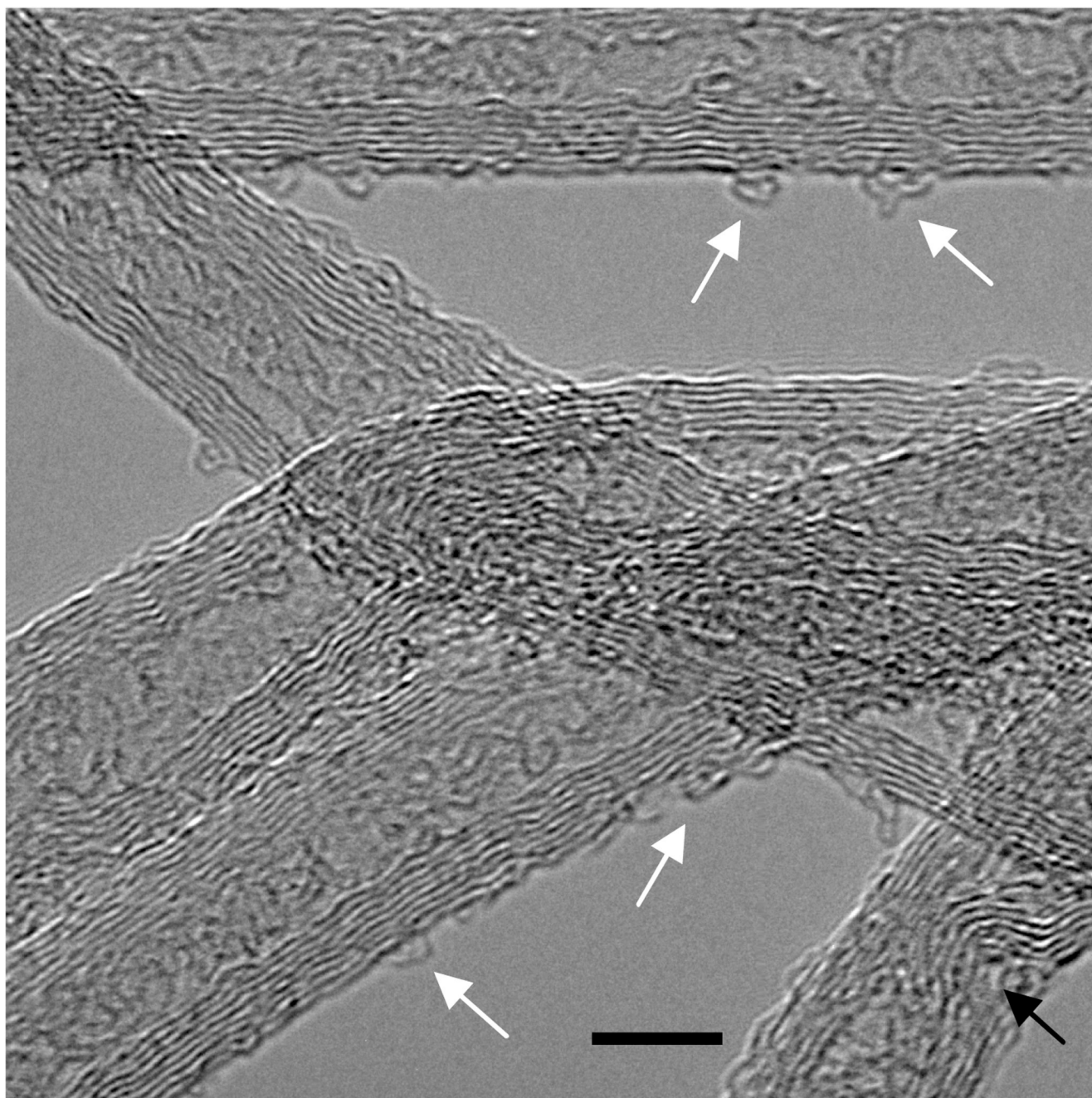


Figure 3.
The HRTEM image of acid-microwaved CNT. The black arrow shows buckling/bending of the graphene sheets and white arrows indicate looping/curling of the surface sheets. The bar represents a distance of 5.0 nm.

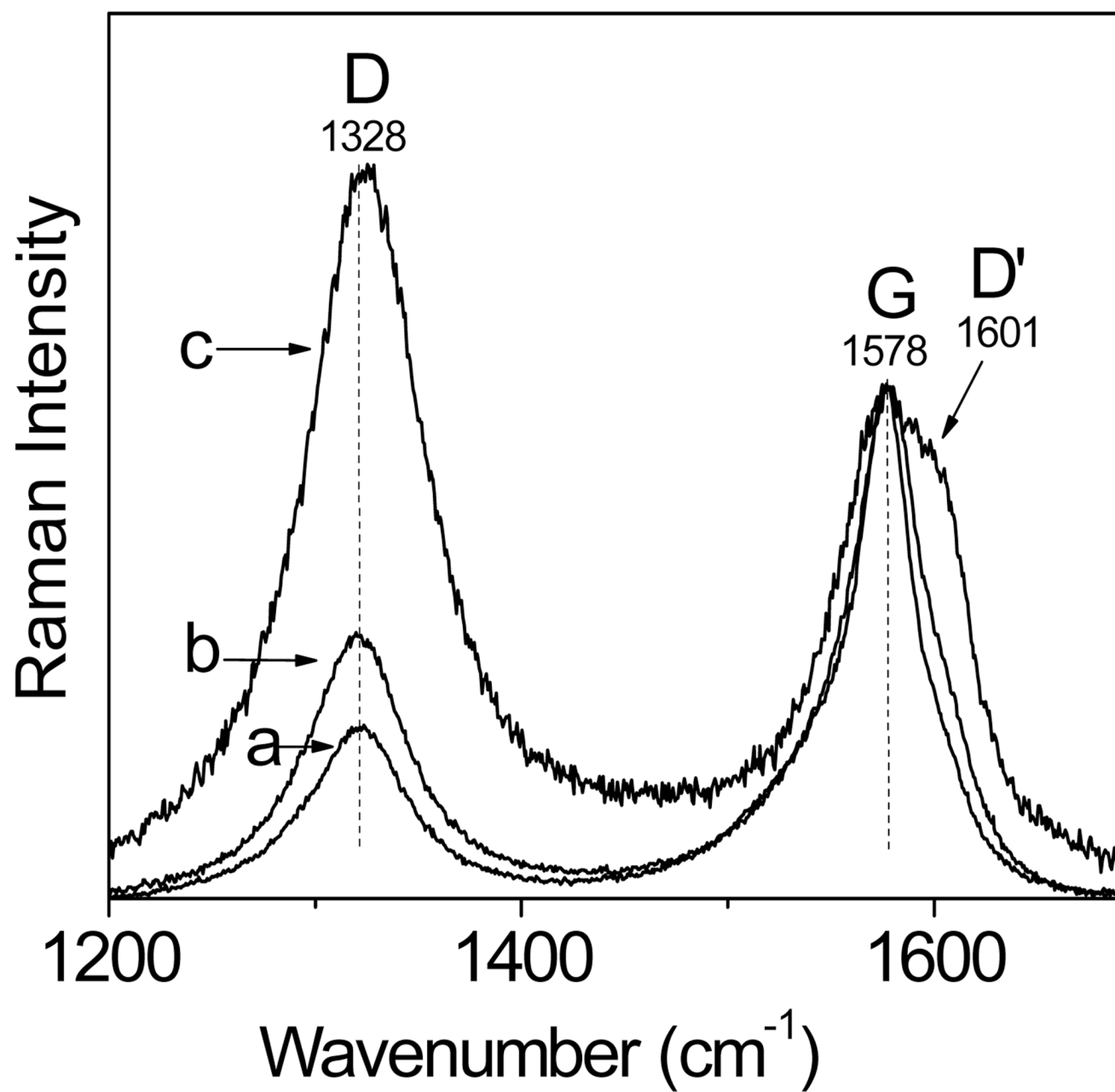


Figure 4. Raman spectra of the original (a), water-boiled (b), and acid-microwaved (c) CNT. The spectra were normalized with respect to the intensity of the G band.

Table 1 E_{NADH} at CNT-based Electrodes (Cyclic Voltammetry, 5.0 mV s^{-1})

Carbon nanotubes	E_{NADH} (V)
As received (original)	0.38 ± 0.03
Boiled in H_2O (10min)	0.10 ± 0.01
Boiled in H_2O (30min)	0.00 ± 0.01
Microwaved in HNO_3 (10min)	-0.04 ± 0.01
Microwaved in HNO_3 (20min)	-0.04 ± 0.01
Sonicated in HNO_3 (20 min)	-0.01 ± 0.01